Arch Toxicol (2008) 82:103–116
DOI 10.1007/s00204-007-0238-x

GENOTOXICITY AND CARCINOGENICITY

Quantitative analysis of liver GST-P foci promoted by a chemical mixture of hexachlorobenzene and PCB 126: implication of size-dependent cellular growth kinetics

Yasong Lu · Manupat Lohitnavy · Micaela Reddy · Ornrat Lohitnavy · Elizabeth Eickman · Amanda Ashley · Lisa Gerjevic · Yihua Xu · Rory B. Conolly · Raymond S. H. Yang

Received: 10 June 2007 / Accepted: 15 August 2007 / Published online: 14 September 2007

Abstract The objectives of this study were twofold: (1) evaluating the carcinogenic potential of the mixture of two persistent environmental pollutants, hexachlorobenzene (HCB) and 3,3′,4,4′,5-pentachlorobiphenyl (PCB 126), in an initiation-promotion bioassay involving the development of π glutathione S-transferase (GST-P) liver foci, and (2) analyzing the GST-P foci data using a biologically-based computer model (i.e., clonal growth model) with an emphasis on the effect of focal size on the growth kinetics of initiated cells. The 8-week bioassay involved a series of treatments of initiator, two-thirds partial hepatectomy, and daily oral gavage of the mixture of two doses in male F344 rats. The mixture treatment significantly increased liver GST-P foci development, indicating carcinogenic potential of this mixture. Our clonal growth model was developed to simulate the appearance and development of initiated GST-P cells in the liver over time. In the model, the initiated cells were partitioned into two subpopulations with the same division rate but different death rates. Each subpopulation was further categorized into single cells, mini- (2–11 cells), medium- (12–399 cells), and large-foci (>399 cells) with different growth kinetics. Our modeling suggested that the growth of GST-P foci is size-dependent; in general, the larger the foci, the higher the rate constants of division and death. In addition, the modeling implied that the two doses promoted foci development in different manners even though the experimental foci data appeared to be similar between the two doses. This study further illustrated how clonal growth modeling may facilitate our understanding in chemical carcinogenic process.

Keywords Hexachlorobenzene · PCB126 · Chemical mixture · Clonal growth model · Liver GST-P foci

Electronic supplementary material The online version of this article (doi:10.1007/s00204-007-0238-x) contains supplementary material, which is available to authorized users.

Y. Lu · M. Lohitnavy · O. Lohitnavy · E. Eickman · L. Gerjevic · R. S. H. Yang (✉)
Quantitative and Computational Toxicology Group,
Department of Environmental and Radiological Health Sciences,
Colorado State University, Fort Collins, CO 80523-1681, USA
e-mail: raymond.yang@colostate.edu

M. Reddy
DMPK Group, Preclinical Sciences,
Roche Palo Alto LLC, CA 94304, USA

A. Ashley
Department of Cell and Molecular Biology,
Colorado State University, Fort Collins, CO 80523, USA

Y. Xu
McArdle Laboratory for Cancer Research,
University of Wisconsin, Madison, WI 53706, USA

R. B. Conolly
National Center for Computational Toxicology, USEPA,
Research Triangle Park, NC 27711, USA

Present Address:
Y. Lu
Translational Pharmacology Group, PDM, Pfizer Inc, Eastern Point Road, Groton, CT 06340, USA

Introduction

During the study of carcinogenesis, preneoplastic foci, visualized by various morphological or immunohistochemical markers, have been widely recognized as precursors of tumors. Given sufficient time, preneoplastic foci may develop into tumors via continuous growth. The

growth of foci has been observed heterogeneous. Grasl-Kraupp et al. (2000) reported that π glutathione S-transferase positive (GST-P) single cells induced by *N*-nitrosomorpholine had lower replication than the cells in multicellular GST-P foci. Buchmann et al. (1994) found that 5-bromo-2′-deoxyuridine (BrdU) incorporation, an index measuring cell replication, in focal nuclei was dependent on focal size in both control and TCDD-treated rats. These qualitative observations, however, cannot provide an understanding from the quantitative perspective in the size-dependency of foci growth.

In the past two decades, efforts have been made to describe preneoplastic foci, especially in the liver, using clonal growth modeling executed by analytical approach (Dewanji et al. 1989; Luebeck et al. 1995; Moolgavkar et al. 1990; Portier et al. 1996) or computer simulation (Conolly and Andersen 1997; Conolly and Kimbell 1994; Ou et al. 2001, 2003; Thomas et al. 2000). As a derivative of the well-known biologically based carcinogenesis model (Moolgavkar et al. 1988), the clonal growth model keeps tracking the growth kinetics of normal and initiated cells, and generates the development of foci over time. As such, any hypothesis regarding the growth of initiated cells can be conveniently plugged into the model and tested by comparison of model output with experimental data. Indeed, Conolly and Andersen (1997) through their modeling exercises suggested that the initiated cells pool induced by diethylnitrosamine (DEN) may consist of two subpopulations (A and B cells) with different growth kinetics. The modeling of Moolgavkar and co-workers (Grasl-Kraupp et al. 2000; Luebeck et al. 1995; Moolgavkar et al. 1996) implied that the growth of GST-P cells in a focus is likely dependent on the focal size. While the size-dependency needs further quantitative exploration, the clonal growth model is likely to serve this purpose.

Although toxicological studies often focus on individual chemicals, human exposure is rarely, if ever, limited to one single chemical (Yang 1994, 1997). Potential interactions among chemicals, at the levels of pharmacokinetics and pharmacodynamics, may modulate the toxicity of each individual. Consequently, it is difficult to accurately predict effects of a chemical mixture solely based on the information of each component. Research on toxicology of chemical mixtures therefore should be encouraged.

Among the numerous chemicals humans are exposed to are two persistent organic pollutants, hexachlorobenzene (HCB) and 3,3′,4,4′,5-pentachlorobiphenyl (PCB 126). They both have been present in the environment (Blais et al. 2003) and in human tissues (Liljegren et al. 1998). Their respective carcinogenicities, along with other toxicities, have been intensively studied. HCB-induced carcinogenicity was observed in laboratory animals with the liver being a main target organ (Erturk et al. 1986; Smith et al. 1985). PCB 126 was reported to significantly increase tumor incidence in multiple sites, e.g., the liver, lung, and oral mucosa, in female Sprague–Dawley rats in a 2-year oral gavage study (NTP 2004). The potential interaction between HCB and PCB 126 has not been addressed so far.

We studied the interaction between HCB and PCB 126 at both pharmacokinetic and pharmacodynamic levels by integrating animal bioassay with computer modeling. The bioassay (Fig. 1), modified from Ito's 8-week protocol (Ito et al. 1989), involved administration of DEN as an initiator, followed by test chemical (HCB, PCB 126, or their mixture in our study) treatment and hepatocyte mitogenic stimulation (partial hepatectomy) in male F344 rats. Tissues were collected for determining chemical concentrations, and liver sections were harvested for measuring GST-P foci as the marker of the pharmacodynamic effect. These measurements were then used to construct physiologically based pharmacokinetic (PBPK) model and clonal growth model, which may provide mechanistic insight into the interaction, if any, between the two chemicals. As a part of that study, this report was focused on (1) evaluating the joint carcinogenic potential of the mixture of HCB and PCB 126 and (2) analyzing the GST-P foci data using a clonal growth model with an emphasis on the size-dependency of the growth kinetics of initiated cells.

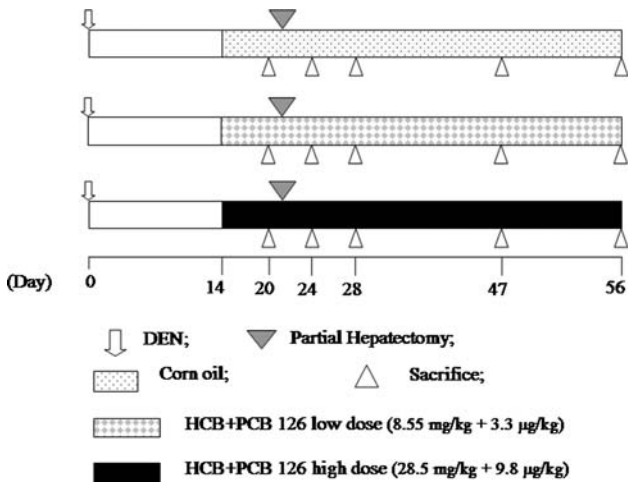

Fig. 1 Experimental design of the time-course medium-term liver foci bioassay. A single i.p. injection of 200 mg/kg DEN was given on day 0. Daily oral gavage of corn oil or HCB + PCB 126 mixture (low or high dose) started from day 14 through sacrifice. On day 21, two-thirds partial hepatectomy was performed on the rats. On the day of surgery and the following 3 days the gavage was suspended to reduce the stress to the animals. Six rats from each treatment group were killed on days 20, 24, 28, 47, and 56. The liver was sectioned and saved appropriately for GST-P foci measurement and other analyses

Materials and methods

Medium-term liver foci bioassay and data collection

Chemicals

HCB (99% purity) was purchased from Aldrich Chemical (Milwaukee, WI). PCB 126 was obtained from Accu-Standard (New Haven, CT). DEN was from Sigma Chemical (St Louis, MO).

Animals and treatment

Male F344 rats, 30 days of age, purchased from Harlan Sprague–Dawley (Indianapolis, IL), were housed in the Painter Center, Colorado State University. It is fully accredited by the American Association for Accreditation of Laboratory Animal Care (AAALAC). Animals were given food (Harlan Teklad NIH-07 diet, Madison, WI) and water ad libitum and lighting was set on a 12 h light/dark cycle.

After 4 weeks of acclimation, the rats were randomized by weight, divided into three groups, and treated according to the time-course medium-term liver foci bioassay (Fig. 1). At week 0, the rats were given a single intraperitoneal (i.p.) injection of DEN (200 mg/kg) in 0.9% saline. Two weeks later, the rats began receiving daily oral gavage of corn oil (control), low dose (8.55 mg/kg + 3.3 μg/kg), and high dose (28.5 mg/kg + 9.8 μg/kg) of HCB + PCB 126 mixture in corn oil until sacrifice. According to the previous work on the individual chemicals in our laboratory (Dean et al. 2002; Ou et al. 2001), 28.5 mg/kg of HCB and 9.8 μg/kg of PCB 126 were expected to cause significant increase in GST-P foci development. The low dose was applied here to examine whether or not it causes significant effect on GST-P foci development given they individually had negligible effects before.

At week 3 (day 21), a two-thirds partial hepatectomy was performed on the rats. On the day of surgery and the following 3 days, the gavage was suspended to reduce the stress to the animals while recovering from surgery. On days 20, 24, 28, 47, and 56, six rats from each treatment group were killed by aortic exsanguination under anesthesia. The body and liver weight of each rat were recorded at sacrifice. A slice of liver was taken along the longest axis of each lobe, fixed in 10% neutral-buffered formalin, embedded in paraffin, and then serially sectioned at thickness of 5 μm. The study was conducted in accordance with the National Institutes of Health (NIH) guidelines for the care and use of laboratory animals.

GST-P foci measurement

Immunohistochemical staining of GST-P foci followed our standard protocol (Ou et al. 2001; Thomas 1998). Foci were measured using a Leitz light microscope coupled with a BioQuant image analysis system (Version 5; R&M Biometrics, Nashville, TN). Foci having two or more cells were recorded.

Hepatocyte proliferation determination

Osmotic minipumps (Alzet model 2ML1, 10 μl/h; Durect Corporation, Cupertino, CA), filled with BrdU (20 mg/ml), were implanted subcutaneously over the dorsal midscapular region 3 days prior to sacrifice. Immunohistochemical detection of BrdU labeled cells followed our standard protocol (Ou et al. 2001; Thomas 1998). At least 1,000 cells/rat and four rats/group were counted. The labeling index (LI), defined as the number of labeled cells divided by the total number of counted cells, was obtained using CHRIS (Version 1.1L; Sverdrup Technology, Fort Walton Beach, FL). The hepatocyte division rate constant (α, 1/day) was calculated using an equation previously proposed (Moolgavkar and Luebeck 1992):

$$\alpha = \frac{1}{2t} \times \ln\left(\frac{1}{1 - \mathrm{LI}}\right), \quad (1)$$

where t is the number of days of exposure to BrdU (t = 3 in our study). This result was seen as the division rate constant of the normal hepatocytes; in this study no effort was made to determine the division rate constant of the cells within foci.

Hepatocyte numerical density quantification

The numerical density (cell number/cm^3) of hepatocyte was represented by the numerical density of hepatocyte nuclei that was evaluated on liver H&E slides. Ten random fields per rat were analyzed. The calculation of numerical density followed the formula reported by Weibel et al. (1969):

$$N_{\mathrm{V}} = \frac{K}{\lambda} \times \frac{N_{\mathrm{A}}^{3/2}}{V_{\mathrm{V}}^{1/2}}, \quad (2)$$

where N_{V} is hepatocyte numerical density, λ is nuclear shape coefficient, K is nuclear size distribution coefficient, N_{A} is number of nuclei per cm^2 test area, and V_{V} is nuclear volume density. In our study, λ = 1.38 according to Weibel and Gomez; K = 1.02 for all groups at day 20, and 1.1 for all groups at other time points accounting for the large

variations in nuclear size (Weibel et al. 1969). The unbiased estimate of V_V is the nuclear area density, i.e., total area of nuclei per cm^2 test area. See Supplemental Material for more details on the derivation of N_A and V_V. The derived numerical density was assumed applicable to both normal and initiated cells.

Stereologic methods

The foci data obtained from liver slides were 2-dimensional (2D) and must be converted to 3-dimensional (3D) expressions for comparison with model outputs. A stereological program by Xu et al. (2003) was used for the conversion. This program uses data containing tissue information (e.g., liver weight and area) and individual focal areas as the input to provide quantitative stereology results on a 3D basis. The outputs include relative foci volume (% liver volume occupied by foci), number of foci/cm^3, and foci size distribution. The theories of the program were detailed in Xu et al. (2003). The relative foci volume was computed by the method of Delesse (1848). Foci number/cm^3 liver was calculated using a modified Saltykov (1967) method, in which 25 size classes were defined. The diameter ratio of two neighboring classes was $10^{-0.1}$. In our study allocation of foci into classes was based on focal volume. At the hepatocyte density of $1.2 \times 10^8/cm^3$, the classes 1–13 were corresponding to cell numbers of 8–16, 17–32, 33–64, 65–127, 128–253, 254–505, 506–1,007, 1,008–2,009, 2,010–4,009, 4,010–8,000, 8,001–15,962, 15,963–31,847, and 31,848–63,543, respectively. The classes 14–25 are omitted here because there were no foci therein.

The focal diameter truncation value (i.e., all foci smaller than that diameter were considered not reliably detectable and thus ignored) for our calculation was set as 63.1 μm for the mixture-treated groups on days 28, 47, and 56, and 50.12 μm for the control group and the first two time points (days 20 and 24) of the mixture groups. The differentiation of the truncation value in different groups and time points was necessary due to hepatocyte enlargement (hypertrophy) after mixture treatment.

Statistical analysis

ANOVA at $\alpha = 0.05$ was applied to analyze statistical differences of the body weight, relative liver weight, hepatocyte numerical density, foci number, and foci area among the control and mixture groups with and without the factor of time. All statistical analyses were performed using SAS (Version 8.02; SAS Institute Inc., Cary, NC).

Clonal growth modeling

Three essential components of the clonal growth model

Growth kinetics of normal hepatocytes The growth of normal hepatocytes was described deterministically by a function of cell division (α, 1/day) and death (β, 1/day) rate constants:

$$\frac{dN}{dt} = N(\alpha - \beta), \tag{3}$$

where N was the number of normal hepatocytes/cm^3 (i.e., hepatocyte numerical density), and β represented different kinds of cell death including apoptosis and necrosis.

Occurrence of initiated cells Initiated cells refer to those cells positive of GST-P staining upon DEN treatment. The occurrence of initiated cells, termed "mutation" in this study, was assumed to be a stochastic process following Poisson distribution. The expected number of initiated cells in a small time step was defined by a function of mutation probability and division rate constant:

$$N_m = N\alpha\mu\Delta t, \tag{4}$$

where N_m is the expected number of initiated cells during a time step Δt, N is normal hepatocyte number/cm^3, and μ is mutation probability per division. A random deviate about N_m denoting the number of initiated cells during Δt was drawn from a Poisson distribution using the strategy by Conolly and Kimbell (1994). Since experiments (Imai et al. 1997; Yusuf et al. 1999) and modeling exercises (Conolly and Andersen 1997; Haag-Gronlund et al. 2000; Ou et al. 2001; Thomas et al. 2000) repetitively suggested heterogeneity of the pool of initiated cells, we assumed that there were two subpopulations (i.e., A and B cells) in the pool, and denoted the mutation probability leading to each subpopulation μ_a and μ_b.

Growth kinetics of initiated cells Once produced, an initiated cell could undergo one of the three random events, i.e., division, death, or no change within a given time step. Growth of initiated cells gave rise to GST-P foci. Death of initiated cells included apoptosis, necrosis, and loss of GST-P phenotype. When a focus was smaller than or equal to 1,000 cells, the growth kinetics of each cell in the clone were treated stochastically according to Conolly and Kimbell (1994). As long as a focus was larger than 1,000 cells, its growth was assumed to be deterministic. The probabilities of division and death were calculated from the rate constants of division (α_a, α_b, 1/day) and death (β_a, β_b,

1/day), respectively (Conolly and Kimbell 1994). The simulation program tracked the behavior of each initiated cell and calculated focal size (cells/focus) and number (foci/cm^3) over time. Divided by hepatocyte numerical density, the total foci size was converted to relative foci volume. The model outputs were 3D and compared to the 3D data converted from the experimental 2D results by the stereologic methods discussed above.

Modeling strategies

Time intervals of piecewise constants The animals in this study were sequentially subjected to three kinds of treatments: DEN (day 0), HCB + PCB 126 mixture dosing (days 14–56), and partial hepatectomy (day 21). These treatments were expected to alter various parameters. Hence, it was necessary to divide the whole simulation duration (56 days) into intervals related to the effects of the treatments. With a modification of the strategy by Ou et al. (2001), we divided the duration into six intervals: days 0–7, 7–14, 14–21.5 (using 21.5 instead of 21 to reflect the lag of 0.5 days between partial hepatectomy and onset of regenerative proliferation, Fukuhara et al. 2003), 21.5–24.5, 24.5–28.5, and 28.5–56. The reasons for designating the first three intervals were discussed in Ou et al. (2001). The split of the duration of days 21.5–28.5 into two intervals was expected to better characterize foci development shortly after partial hepatectomy. The parameters related to growth of initiated cells were fixed within each interval and varied among different intervals.

Detection limit of foci In the 2D analysis, all foci having two or more cells were counted. During the 2D to 3D conversion, the influence of chemical-induced hepatocyte enlargement was incorporated. Our calculation using the information of hepatocyte density and diameters of 2-cell foci in a 2D setting suggested that the 3D detection limit was $\sim$8 cells at all time. Therefore, any focus smaller than 8 cells in the 3D setting were treated undetectable; otherwise it was detectable and contributed to the final simulation outputs.

Size-dependent growth kinetics Our preliminary modeling analyses showed that the size distribution of foci could not be described well without considering the impact of size on cell kinetics. Thus, we hypothesized that the growth kinetics of GST-P foci promoted by HCB + PCB 126 mixture were dependent on focal size. We divided the foci in both A and B subpopulations into several categories in terms of size and each category had specific growth kinetic characteristics. In general, the larger the foci, the higher the rate constants of division and death. This strategy represented an improvement of our current modeling over the earlier ones (Conolly and Andersen 1997; Haag-Gronlund et al. 2000; Ou et al. 2001; Thomas et al. 2000) where the growth kinetics of initiated cells were assumed independent of focal size.

Parameterization

Division and death rate constants of normal hepatocytes The division rate constant of normal hepatocytes was obtained from experiments. Prior to the regenerative proliferation due to partial hepatectomy (day 21.5), the time-course division rate constant was calculated using Eq. 1 with BrdU LI data from Kato et al. (1993a) as well as results from our bioassay (day 20 data). The results were formulated into empirical functions to describe the division rate constant over time until day 21.5. On day 21.5, the division rate constant was set at 0.40/day to account for the proliferation surge due to partial hepatectomy (Ou et al. 2001, 2003). Thereafter, the constant during the segments of days 21.5–24, 24–28, 28–47, and 47–56 was derived from our BrdU LI data that were obtained on days 24, 28, 47, and 56.

The death rate constant, not experimentally obtainable, was related to the total hepatocyte number and division rate constant as shown in Eq. 3. The total hepatocyte number was inferred by liver weight and hepatocyte density. Prior to day 6, the death rate constant was described by a function fitting to the time course liver weight after an i.p. injection of 150 mg/kg DEN reported by Kato et al. (1993a). Thereafter, the death rate constant was equal to a background value, which was set the same as the lowest division rate constant, 8.6×10^{-4}/day, determined in the control group in our bioassay. The rationale for this choice was that the death rate constant was presumably stable 6 days after DEN treatment and that the rate constants of death and division were similar when the liver weight was not changing significantly with time. For the high dose group following day 28, the death rate constant was set twofold higher than the background, accounting for the cytotoxicity of the mixture treatment.

Mutation probability In this study, the mutation probability comprised of two portions: the background level and, more importantly, the increased level due to DEN treatment. The background mutation probability was set at 1.7×10^{-6}/division for both A and B cells (Ou et al. 2001). The strategy of determining the increase over the background was different from the earlier approach, in which

the increase was calibrated with experimental foci number (Conolly and Andersen 1997; Conolly and Kimbell 1994; Ou et al. 2001). Since not all initiated cells give rise to detectable foci (Grasl-Kraupp et al. 2000; Kato et al. 1993b), the earlier approach might give an underestimated mutation probability. To alleviate this drawback, we set the increased fold at a level that produced $\sim 10^4$ initiated cells per cm^3 of liver (Haag-Gronlund et al. 2000; Luebeck et al. 2000; Satoh et al. 1989). Since only a small percentage (5–23%) of the foci generated by DEN was resistant to selective mitoinhibitory pressures (Yusuf et al. 1999), in our modeling, the ratio of the mutation probabilities generating A and B cells was assumed to be 10:1 (μ_a:μ_b = 10:1) (Table 3). After partial hepatectomy, transient increases in both μ_a and μ_b from the background levels were employed for insufficient monitoring and repairing of genetic or epigenetic alterations that lead to GST-P expression.

Categorization and division and death rate constants of foci To relate cellular kinetics to focal size, the A and B foci were both categorized according to their sizes. Note that here the categories were different from the size classes introduced earlier. The categorization dividers were selected on the basis of two criteria: (1) to be in line with the current understanding in the growth kinetics of initiated cells (Grasl-Kraupp et al. 2000), and (2) to replicate the size distribution patterns through computer simulations. Each category had distinct growth kinetics. To reduce the number of unknown parameters, we assigned A and B cells with the same division rate constant in each category within each time interval. The death rate constant of A cells was generally assumed to be higher than that of B cells, reflecting the higher sensitivity of A cells to the selective mitoinhibitory pressure (Conolly and Andersen 1997; Yusuf et al. 1999). We adjusted the category dividers and the cellular division and death rate constants to simulate three pieces of data simultaneously: relative foci volume, foci number/cm^3, and size distribution.

More technical details of the model implementation were introduced earlier (Conolly and Andersen 1997; Conolly and Kimbell 1994; Ou et al. 2001, 2003; Thomas et al. 2000). The model presented here is parameter-rich; however, all parameters were from the literature, our bioassay, or calibration to our foci data as discussed above. Because of the stochasticity of the growth of initiated cells, the model was run for 20 times; the averages of the 20 runs were compared to our data for calibration.

Software

The clonal growth model was coded and the simulations were performed using ACSL Tox 11.8.4 (AEgis Technologies Group, Huntsville, AL).

Results

Experimental data collection

Effect of the mixture treatment on the body and liver weight and liver section area

No rat died of the mixture treatment. The body weights of the mixture treated rats significantly reduced in a dose-dependent manner on days 47 and 56; on day 28 the reduction was significant only in the high dose group (data not shown). Significant increase in the liver weight of the two mixture groups over the control group was observed on days 28, 47, and 56, but there was no difference between the two mixture groups (Fig. 2a). The relative liver weight (% body weight) was almost doubled by the mixture treatment from day 28 onward and the increase was dose dependent (Fig. 2b). In agreement with the increase in the

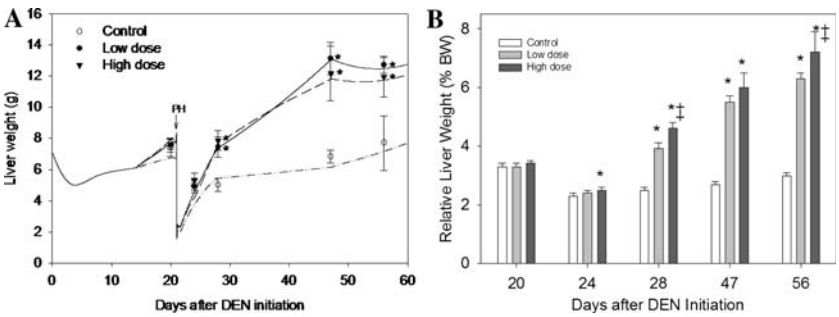

Fig. 2 **a** Time-course liver weight recorded in the experiment and simulated by the clonal growth model. The *symbols* are experimental data and the *curves* are model simulations. The *arrow* indicates when the partial hepatectomy (PH) was performed. **b** Time-course relative liver weight (% body weight, *BW*) in the control and mixture treated groups. *Significantly different ($P < 0.05$) from the concurrent control group; ‡Significantly different ($P < 0.05$) from the concurrent low dose group

Table 1 Time-course liver section area, hepatocyte division rate constant, and hepatocyte numerical density in the medium-term liver foci bioassay

Treatment	Day 20	Day 24	Day 28	Day 47	Day 56
Liver section area[a] (cm^2)					
Control	2.89 ± 0.48	3.69 ± 0.11	3.65 ± 0.38	4.43 ± 0.25	4.22 ± 0.62
Low dose	2.39 ± 0.40	3.92 ± 0.51	4.61 ± 0.54*	7.12 ± 0.82*	6.92 ± 0.32*
High dose	2.58 ± 0.49	4.00 ± 0.35	4.81 ± 0.57*	6.28 ± 0.85*	6.07 ± 0.63*
Hepatocyte division rate constant (α, $\times 10^{-3}$/day)					
Control	2.3 ± 0.8	113.4 ± 23.4	7.3 ± 5.1	0.9 ± 0.5	1.1 ± 0.4
Low dose	2.4 ± 1.3	130.0 ± 59.7	14.9 ± 9.0	0.8 ± 0.8	3.7 ± 3.5
High dose	2.5 ± 1.7	126.4 ± 43.2	27.7 ± 10.0**	3.5 ± 2.9**	14.2 ± 6.9**
Hepatocyte density ($\times 10^8/cm^3$)					
Control	1.10 ± 0.17	1.20 ± 0.08	1.10 ± 0.11	1.20 ± 0.01	1.00 ± 0.01
Low dose	0.99 ± 0.16	0.99 ± 0.06	0.83 ± 0.01*	0.57 ± 0.02*	0.64 ± 0.02*
High dose	0.97 ± 0.18	1.10 ± 0.12	0.81 ± 0.08*	0.60 ± 0.16*	0.64 ± 0.06*

The results were expressed as mean ± SD

* Significantly different from the concurrent control group, $P < 0.05$

** Significantly different from the concurrent other groups, $P < 0.05$

[a] Each slice of liver was taken along the longest axis of each lobe. Thus, the increase in liver section area indicated the enlargement of liver

liver weight, the area of the liver section was also increased on days 28, 47, and 56 with no difference between the two mixture groups (Table 1).

Hepatocyte division rate constant

The hepatocyte division rate constant (Table 1) was calculated from experimentally derived LI. On day 24, the constant was around 0.12/day for all groups; this division rate was about 50-fold higher than that on day 20. This remarkable elevation reflected the regenerative cell proliferation following the partial hepatectomy on day 21. After day 24, a great reduction was observed. On day 28, the division rate constant in the high dose group was 0.028/day, two- and fourfold higher than that in the low and control group, respectively. The index in all groups was further reduced on day 47, but somewhat increased again at the last time point, day 56. At the late three time points, days 28, 47, and 56, the constant was generally dose-related, i.e., the higher dose led to higher division rate constant.

Hepatocyte numerical density

The hepatocyte numerical density of a naive adult F344 rat determined using our method was $1.2 \times 10^8/cm^3$, which was close to the values reported in the literature (Moolgavkar et al. 1990; Weibel et al. 1969). The mixture treatment caused hepatocyte enlargement with concomitant numerical density reduction as shown in Table 1. The reduction on days 28, 47, and 56 of both mixture groups was significant relative to the control group, yet the difference between the mixture groups was not significant. The change in hepatocyte numerical density was incorporated in our modeling.

2D GST-P foci data

The foci formation was measured by total foci area and foci number identified from the GST-P stained liver slides. We analyzed these measurements with and without the standardization by the liver area, in order to examine the impact of liver enlargement (25–65% larger than control) on the results.

Without the standardization, the total foci areas in all groups, shown in Fig. 3a, increased with time. At the first time point, there was no difference among all groups. On day 24, the foci area in the high dose group was significantly increased compared to the other two groups. Thereafter, the foci areas of the two mixture groups, not different from each other, were significantly higher (2–3 fold) than that of the control. The foci number in the control group remained around 50–60/liver at all time points (Fig. 3b). In the first week after partial hepatectomy, the number notably increased (roughly threefold) in both mixture groups. Thereafter, it was relatively stable until day 56.

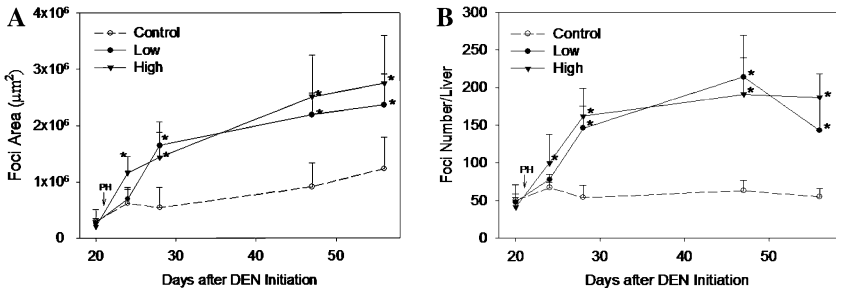

Fig. 3 Time-course foci area (**a**) and foci number (**b**) measured from the liver slides of the rats treated with corn oil or HCB + PCB 126 mixture. The *arrows* indicate when the partial hepatectomy (PH) was performed. *Significantly different ($P < 0.05$) from the concurrent control group; ‡Significantly different ($P < 0.05$) from the concurrent low dose group

When the foci area and foci number were standardized by the liver area, the difference between the control and the mixture groups remained statistically significant ($P < 0.05$) with one exception; on day 56, the relative foci area in the low dose group was not significantly different from the control. The magnitude of the difference among the groups was somewhat diminished.

3D GST-P foci data

The slide-derived 2D measurements were converted to 3D expressions for calibrating the clonal growth model. The conversions provided the data of relative foci volume (Fig. 4a, c, e), foci number/cm^3 liver (Fig. 4b, d, f), and size distribution (Table 2). The foci in the mixture

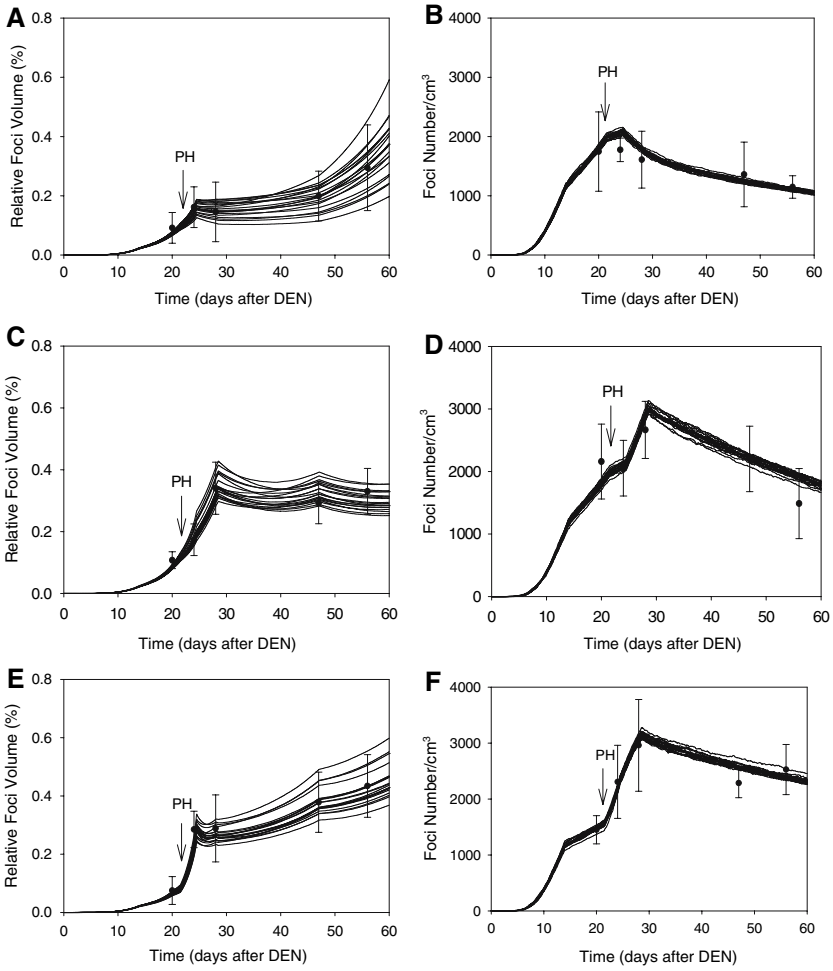

Fig. 4 Experimental and simulated time-course foci relative volume and foci number/cm^3 in the control (**a**, **b**), low dose (**c**, **d**), and high dose (**e**, **f**) groups. The *symbols* are data converted from the experimental 2D results and the *curves* are model simulations of 20 runs. The *arrows* indicate when the partial hepatectomy (PH) was performed

Table 2 Experimental and simulated 3-dimensional foci size distribution (number of foci/class)

Treatment	Size class	Time points									
		Day 20		Day 24		Day 28		Day 47		Day 56	
		Data	*Model*	Data	*Model*	Data	*Model*	Data	*Model*	Data	*Model*
Control	1	764	*602*	626	*569*	483	*455*	361	*203*	208	*148*
	2	458	*442*	412	*448*	548	*419*	339	*362*	276	*315*
	3	310	*391*	234	*415*	316	*407*	267	*334*	291	*314*
	4	167	*247*	253	*352*	155	*296*	133	*208*	136	*200*
	5	24	*103*	149	*194*	46	*146*	113	*72*	126	*73*
	6	67	*24*	51	*61*	38	*18*	57	*20*	35	*28*
	7	26	*3*	30	*11*	17	*13*	26	*15*	31	*18*
	8	0	*1*	23	*8*	17	*10*	24	*9*	20	*16*
	9	0	*0*	0	*4*	3	*6*	18	*9*	14	*7*
	10	0	*0*	1	*1*	3	*3*	3	*4*	7	*6*
	11	0	*0*	0	*0*	1	*1*	0	*2*	7	*4*
	12	0	*0*	0	*0*	0	*0*	0	*1*	0	*2*
	13	0	*0*	0	*0*	0	*0*	0	*0*	0	*0*
Low	1	893	*692*	739	*689*	–[a]	–	–	–	–	–
	2	474	*430*	477	*393*	903	*828*	803	*607*	523	*519*
	3	397	*382*	369	*438*	748	*444*	548	*523*	355	*432*
	4	197	*289*	221	*382*	450	*423*	410	*461*	244	*348*
	5	72	*122*	104	*242*	306	*357*	229	*311*	150	*243*
	6	50	*38*	64	*96*	128	*215*	146	*158*	114	*96*
	7	23	*5*	32	*12*	71	*82*	47	*90*	63	*115*
	8	0	*2*	20	*10*	43	*11*	28	*44*	36	*42*
	9	0	*1*	2	*5*	4	*9*	7	*3*	6	*2*
	10	0	*0*	2	*3*	1	*5*	2	*3*	7	*3*
	11	0	*0*	0	*1*	1	*2*	0	*1*	1	*1*
	12	0	*0*	0	*0*	0	*1*	0	*1*	1	*1*
	13	0	*0*	0	*0*	0	*0*	0	*0*	0	*0*
High	1	635	*626*	670	*668*	–	–	–	–	–	–
	2	396	*282*	552	*356*	1,207	*1,137*	866	*928*	759	*759*
	3	232	*341*	421	*304*	739	*324*	580	*490*	776	*429*
	4	130	*242*	378	*294*	540	*294*	323	*402*	458	*338*
	5	74	*93*	133	*325*	230	*328*	257	*425*	240	*344*
	6	11	*26*	84	*181*	148	*258*	100	*225*	176	*253*
	7	11	*2*	45	*67*	33	*32*	96	*46*	86	*70*
	8	0	*1*	38	*15*	20	*18*	24	*32*	30	*45*
	9	3	*0*	18	*3*	0	*7*	14	*18*	21	*19*
	10	0	*0*	2	*1*	0	*2*	3	*7*	2	*9*
	11	0	*0*	0	*1*	0	*0*	1	*1*	0	*2*
	12	0	*0*	0	*0*	1	*0*	1	*0*	2	*0*
	13	0	*0*	0	*0*	0	*0*	0	*0*	0	*0*

The simulations (*Model*) were averages of 20 runs of the clonal growth model

[a] In the low and high dose groups on days 28, 47, and 56, due to cell hypertrophy, the class 1 was equivalent to the class 2 at other time points in terms of focal volume and hence was placed in the line of class 2, and likewise for the larger classes

groups were shifted to larger classes (i.e., larger foci) compared to those in the control group, suggesting the promotion effect of the mixture treatment. Between the two mixture groups the distribution patterns were similar.

It is interesting to note that the development of GST-P foci, in terms of area, number, and size distribution, was similar between the two mixture groups even though there was a threefold difference between the dose levels (HCB 8.55 mg/kg + PCB 126 3.3 μg/kg vs. HCB 28.5 mg/kg + PCB 126 9.8 μg/kg).

Clonal growth model simulations

Calibration of hepatocyte death rate constant

The hepatocyte death rate constant was calibrated using the time-course experimental liver weight. As shown in Fig. 2a, the liver weight was simulated well with the experimentally derived division rate constant and the calibrated death rate constant. At the beginning of simulation, the death rate constant was at a background level (8.6×10^{-4}/day). After 0.1 days, the lag between DEN exposure and the onset of cytotoxicity, the death rate constant peaked to 0.15/day, and linearly declined until day 6.1 to the background. Thereafter the death rate constant was held at the background level, with the exception that it was doubled after day 28 in the high dose group to account for the cytotoxicity of the mixture treatment.

Simulation of the foci data

As a tradeoff between model parsimony and adequate simulation of data (especially size distribution), the foci were placed into four categories: single cell, minifoci (2–11 cells), medium-foci (12–399 cells), and large-foci (>399 cells). Note that the categories were introduced for characterizing the growth kinetics of initiated cells, and should be distinguished from the size classes (see Table 2 for size classes). A direct comparison of the categories and size classes is as follows: the single cells were too small to be in any size class, the minifoci category covered the lower portion of class 1, the medium-foci category covered the upper portion of class 1 through the lower portion of class 6, and the large-foci category covered the other classes.

Our model simulations of the relative foci volume and foci number/cm^3 were consistent with the experimental data (Fig. 4). Furthermore, the size distribution patterns of all groups were also well simulated as shown in Table 2. In the control group, the foci numbers in the smaller classes gradually decreased, and the distribution of all foci shifted toward the larger classes in the later time points. In the mixture groups, the foci also became larger with time; moreover, the numbers in the smaller classes were remarkably increased from day 28 onwards compared to the concurrent control.

Parameters related to initiated cells and foci development

The mutation probabilities (μ_a, μ_b) and rate constants for division (α_a, α_b) and death (β_a, β_b) of initiated cells calibrated with the data are listed in Table 3. While the division rate constants (α_a's, α_b's) of mini-, medium-, and large-foci were determined by simulating the experimental data, those for single cells were assigned with theoretical values because of the lack of reliable data on single cells. Thus, the division rate constants for single cells were assumed to be independent of the mixture treatment and the values assigned were lower than those for normal cells. The latter is supported by the earlier finding (Grasl-Kraupp et al. 2000) that the LI of the GST-P single cells was lower than that of normal hepatocytes after injection of [^{3}H]-thymidine in the rat. In general, the α_a and α_b in our study, being set equal, had trends of gradual decrease over time and increase with focal size. After partial hepatectomy, the mixture treatment, especially the high dose, remarkably stimulated the division of cells in minifoci (α's increased), which contributed to the significant increase in the foci number in the smaller classes. The higher division rate constants of medium-foci in the mixture groups led to the increase in the relative foci volume and size distribution shift. The division of large foci, however, was less affected by the mixture treatment. The β_a was set higher than β_b, reflecting the higher sensitivity of A cells to a selective mitoinhibitory pressure as observed earlier (Conolly and Andersen 1997; Yusuf et al. 1999). Upon the mixture treatment, the sensitivity of A cells were further elevated and that of B cells was inhibited. As a result, the ($\alpha_b - \beta_b$) was generally higher than ($\alpha_a - \beta_a$), especially after day 24.5, reflecting the enhancement of the growth advantage of B cells by the mixture treatment.

The effects of the mixture dose on α's, β's, and ($\alpha - \beta$)'s were not always consistent and they were dependent on focal size and time. In the first week following partial hepatectomy (days 21.5–28.5), the division rate constants and the net growth rate ($\alpha_b - \beta_b$) of mini- and medium-foci were notably different between the low and high dose groups (Table 3).

Discussion

HCB + PCB 126 promotion of GST-P foci

In our time-course medium-term bioassay, the HCB + PCB 126 mixture treatment significantly elevated the foci

Table 3 Division and death rate constants of initiated cells and normal cell mutation probabilities in the clonal growth model

Parameter	Foci category	Treatment	Simulation interval (days)					
			0–7	7–14	14–21.5	21.5–24.5	24.5–28.5	28.5–56
α_a, α_b (1/day)	Single cell	Control	0.03	0.012	0.02	0.004	0.001	0.001
		Low	0.03	0.012	0.02	0.004	0.001	0.001
		High	0.03	0.012	0.02	0.004	0.001	0.001
	Minifoci	Control	0.3	0.22	0.11	0.09	0.08	0.1
		Low	0.3	0.22	0.11	0.099	0.192	0.175
		High	0.3	0.22	0.055	0.27	0.24	0.17
	Medium-foci	Control	0.41	0.35	0.2	0.17	0.17	0.1
		Low	0.41	0.35	0.2	0.17	0.315	0.138
		High	0.41	0.35	0.2	0.476	0.187	0.12
	Large-foci	Control	0.42	0.42	0.42	0.4	0.25	0.1
		Low	0.42	0.42	0.42	0.4	0.25	0.095
		High	0.42	0.42	0.42	0.472	0.25	0.07
β_a (1/day)	Single cell	Control	0.0008	0.0008	0.0008	0.002	0.0005	0.0001
		Low	0.0008	0.0008	0.0008	0.002	0.0005	0.0001
		High	0.0008	0.0008	0.0008	0.002	0.0005	0.0001
	Minifoci	Control	0.0008	0.0008	0.0015	0.07	0.18	0.18
		Low	0.0008	0.0008	0.0015	0.07	0.045	0.216
		High	0.0008	0.0008	0.0033	0.07	0.126	0.18
	Medium-foci	Control	0.0008	0.05	0.04	0.06	0.28	0.12
		Low	0.0008	0.05	0.04	0.06	0.224	0.184
		High	0.0008	0.05	0.072	0.06	0.28	0.144
	Large-foci	Control	0.0008	0.01	0.01	0.01	0.2	0.09
		Low	0.0008	0.01	0.01	0.01	0.22	0.198
		High	0.0008	0.01	0.01	0.01	0.64	0.27
β_b (1/day)	Single cell	Control	0.00008	0.00008	0.00008	0.001	0.0005	0.0001
		Low	0.00008	0.00008	0.00008	0.001	0.0005	0.0001
		High	0.00008	0.00008	0.00008	0.001	0.0005	0.0001
	Minifoci	Control	0.00008	0.00008	0.00008	0.02	0.13	0.15
		Low	0.00008	0.00008	0.00008	0.02	0.013	0.09
		High	0.00008	0.00008	0.00008	0.02	0.026	0.075
	Medium-foci	Control	0.00008	0.0008	0.0008	0.02	0.23	0.06
		Low	0.00008	0.0008	0.0008	0.02	0.138	0.057
		High	0.00008	0.0008	0.0008	0.02	0.23	0.024
	Large-foci	Control	0.00008	0.0008	0.0008	0.01	0.16	0.04
		Low	0.00008	0.0008	0.0008	0.01	0.16	0.082
		High	0.00008	0.0008	0.0008	0.01	0.16	0.046
μ_a ($\times 1.7 \times 10^{-6}$)			350	20	1	5	2	1
μ_b ($\times 1.7 \times 10^{-6}$)			35	2	1	5	2	1

number/liver and foci area starting from day 28 compared to the concurrent control. The foci number was tripled and the foci area was doubled. Both HCB (Cabral et al. 1996; Ou et al. 2001) and PCB 126 (Bager et al. 1995; Dean et al. 2002) alone were reported to promote the growth of altered hepatic foci in rats, hence it is not surprising to observe the promotional effect of the mixture of these two chemicals.

There was a threefold difference between the low (HCB 8.55 mg/kg + PCB 126 3.3 μg/kg) and high (HCB 28.5 mg/kg + PCB 126 9.8 μg/kg) dose levels. Interestingly, the development of GST-P foci, in terms of area, number, and size distribution, was not significantly different between the two mixture groups. In our previous study with the same protocol, PCB 126 at the level of

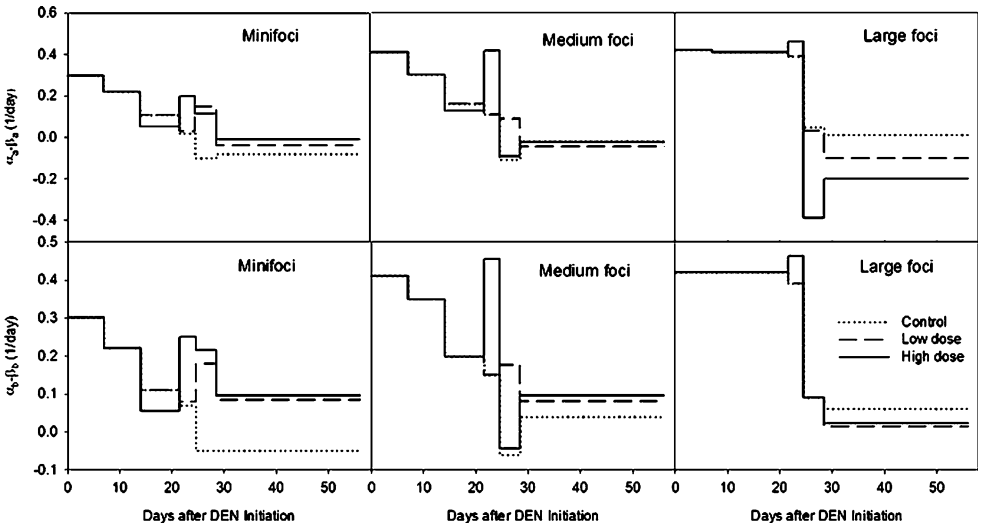

Fig. 5 The growth kinetic parameters, $\alpha_a - \beta_a$ (*upper panels*) and $\alpha_b - \beta_b$ (*lower panels*), of A and B cells in the mini-, medium, and large foci derived from the clonal growth model

9.8 μg/kg significantly promoted the development of GST-P foci, but at the level of 3.3 μg/kg the effect was not significant (Lohitnavy et al., unpublished data). HCB only significantly increased the foci number on day 56 at 28.5 mg/kg; at 8.55 mg/kg the effect was insignificant (Lu et al., unpublished data). These results imply the possibility of synergistic interaction between HCB and PCB 126 at the low dose in this study. Further studies are needed (1) to explore the mechanism(s) of the interaction between these two chemicals, and (2) to examine the promotion potency of the mixture at even lower doses.

Although the low and high dose treatments yielded similar observations, the kinetic parameters ($\alpha_a - \beta_a$ and $\alpha_b - \beta_b$) of the initiated cells and foci, according to our modeling analyses, were dose dependent, especially in the intervals following partial hepatectomy, as shown in Fig. 5. This result suggests that the development of GST-P foci may be dose-dependent, even though the dependency was not observable at the level of foci areas or numbers. It also illustrates one of the powerful utilities of the clonal growth modeling in generating hypothesis.

Size-dependent growth kinetics of GST-P foci

The most notable finding in this current study was that the growth kinetics of GST-P foci depended on focal size. To describe the data of foci size distribution successfully, the influence of focal size on the division and death rate constants had to be taken into account. We grouped the foci into four categories according to the focal sizes. In our model, the net growth rates of both A and B types of foci were generally increased with focal size. This result is in good agreement with our current understanding in clonal growth.

The expansion of foci is a result of continuous competition between the growth capability of initiated cells and the homeostatic control mechanisms. One of such mechanisms is gap junctional intercellular communication (GJIC) (Omori et al. 2001), which exists among initiated and surrounding normal cells (heterologous GJIC) and among initiated cells (homologous GJIC) (Krutovskikh 2002). GJIC organizes cells in a society and places each cell under the monitoring of all the neighboring cells. When an initiated hepatocyte appears, it is effectively monitored by its neighbors and its proliferation is checked by receiving growth-controlling signals through gap junctions (Krutovskikh 2002). This is one of the reasons why the division rate constant of single cells in our model was set very low compared to that of the other categories. GJIC is likely to be inhibited by chemicals, e.g., HCB (Plante et al. 2002), PCB 126 (Bager et al. 1997), and thus the single cells are somewhat released from proliferation check. This effect was not embodied in our study due to lack of necessary data.

When single cells become foci with multiple cells, the proliferation check via heterologous GJIC from normal cells is lessened because on average each initiated cell is surrounded by fewer normal cells. Chemical treatments such as HCB (Plante et al. 2002) and PCB 126 (Bager et al. 1997) may further reduce the proliferation check. Meanwhile, the initiated cells may share factors via the homologous GJIC counterbalancing growth-controlling signals. These two aspects, in combination, stimulate replication of initiated cells in foci. With the increase in focal size, the growth control is further abolished and focal expansion becomes more autonomous, reflected by the higher net growth rates in larger foci observed in our study. Krutovskikh (2002) suggested a dynamic process of focal expansion and GJIC inhibition. Given GJIC is a basic

homeostatic mechanism, it is likely that the focal size-dependent promotion by HCB + PCB 126 mixture is also applicable to other tumor promoters.

Model configuration and parameterization

Our clonal growth model had a structure with two compartments, hepatocytes and initiated cells. The change of each compartment and the transition from hepatocytes to initiated cells were described by dynamic functions. The functions, along with the pertinent parameters, were assigned on the basis of educated guess and experimental data. Since our current knowledge was too limited to determine how accurately the functions and parameters captured the reality, the model should be recognized as a semi-quantitative rather than a fully quantitative model. As such, in this study, we focused on the question of "what can we learn from the model?" rather than "what predictions can we make using the model?"

The parameterization in a carcinogenesis model using tumor incidence data has been facing several statistical difficulties, including parameter nonidentifiability and nonestimability and model nondifferentiability. In a clonal growth model, however, some of the difficulties may be alleviated to certain degree because of the much more information contained in a foci dataset. The foci size constrains the value of the difference between the division and death rate constant, and the foci number constrains the values of the individual constants (Dewanji et al. 1989). During our parameterization, all division and death rate constants were constrained by the foci size, number, and size distribution simultaneously, and thus our parameter set is likely to be unique. Indeed, we could not find another set fitting the three pieces of data equally well at the same time.

In summary, in the current study, HCB + PCB 126 mixture significantly promoted GST-P foci formation in the context of a medium-term liver foci bioassay. We constructed a clonal growth model to describe the experimental foci data with special emphasis on the size dependency of the foci growth kinetics with or without the presence of the mixture. The data were well simulated by our model, which supported our hypothesis of size-dependent foci growth kinetics. While the data showed that the promotional effects were similar between the low and high doses regardless of the threefold difference, the model implied that the two doses stimulated foci growth in different manners.

Acknowledgments This study is supported by the NIOSH/CDC grant 1 RO1 OH07556, NIEHS Training Grant 1 T32 ES 07321, and scholarships from U.S. Fulbright Foundation and Naresuan University, Thailand. The authors thank Dr. Ying C. Ou for her help with the computer code and thank Ms. Traci Nichols, Drs. Todd Painter and Charles Dean, and other colleagues in the Quantitative and Computational Toxicology Group for their excellent technical assistance. The support on statistical analysis of the experimental data from Dr. Xiaohui Xu is greatly appreciated.

References

Bager Y, Hemming H, Flodstrom S, Ahlborg UG, Warngard L (1995) Interaction of 3,4,5,3′,4′-pentachlorobiphenyl and 2,4,5,2′,4′,5′-hexachlorobiphenyl in promotion of altered hepatic foci in rats. Pharmacol Toxicol 77:149–154

Bager Y, Kato Y, Kenne K, Warngard L (1997) The ability to alter the gap junction protein expression outside GST-P positive foci in liver of rats was associated to the tumour promotion potency of different polychlorinated biphenyls. Chem Biol Interact 103:199–212

Blais JM, Froese KL, Kimpe LE, Muir DC, Backus S, Comba M, Schindler DW (2003) Assessment and characterization of polychlorinated biphenyls near a hazardous waste incinerator: analysis of vegetation, snow, and sediments. Environ Toxicol Chem 22:126–133

Buchmann A, Stinchcombe S, Korner W, Hagenmaier H, Bock KW (1994) Effects of 2,3,7,8-tetrachloro- and 1,2,3,4,6,7,8-heptachlorodibenzo-p-dioxin on the proliferation of preneoplastic liver cells in the rat. Carcinogenesis 15:1143–1150

Cabral R, Hoshiya T, Hakoi K, Hasegawa R, Ito N (1996) Medium-term bioassay for the hepatocarcinogenicity of hexachlorobenzene. Cancer Lett 100:223–226

Conolly RB, Andersen ME (1997) Hepatic foci in rats after diethylnitrosamine initiation and 2,3,7,8-tetrachlorodibenzo-p-dioxin promotion: evaluation of a quantitative two-cell model and of CYP 1A1/1A2 as a dosimeter. Toxicol Appl Pharmacol 146:281–293

Conolly RB, Kimbell JS (1994) Computer simulation of cell growth governed by stochastic processes: application to clonal growth cancer models. Toxicol Appl Pharmacol 124:284–295

Dean CE Jr, Benjamin SA, Chubb LS, Tessari JD, Keefe TJ (2002) Nonadditive hepatic tumor promoting effects by a mixture of two structurally different polychlorinated biphenyls in female rat livers. Toxicol Sci 66:54–61

Delesse M (1848) Procede mecanique pour determiner la composition des roches. Ann Mines 13:379–388

Dewanji A, Venzon DJ, Moolgavkar SH (1989) A stochastic two-stage model for cancer risk assessment. II. The number and size of premalignant clones. Risk Anal 9:179–187

Erturk E, Lambrecht RW, Peters HA, Cripps DJ, Gocmen A, Morris CR, Bryan GT (1986) Oncogenicity of hexachlorobenzene. IARC Sci Publ 77:417–423

Fukuhara Y, Hirasawa A, Li XK, Kawasaki M, Fujino M, Funeshima N, Katsuma S, Shiojima S, Yamada M, Okuyama T, Suzuki S, Tsujimoto G (2003) Gene expression profile in the regenerating rat liver after partial hepatectomy. J Hepatol 38:784–792

Grasl-Kraupp B, Luebeck G, Wagner A, Low-Baselli A, de Gunst M, Waldhor T, Moolgavkar S, Schulte-Hermann R (2000) Quantitative analysis of tumor initiation in rat liver: role of cell replication and cell death (apoptosis). Carcinogenesis 21:1411–1421

Haag-Gronlund M, Conolly R, Scheu G, Warngard L, Fransson-Steen R (2000) Analysis of rat liver foci growth with a quantitative two-cell model after treatment with 2,4,5,3′,4′-pentachlorobiphenyl. Toxicol Sci 57:32–42

Imai T, Masui T, Ichinose M, Nakanishi H, Yanai T, Masegi T, Muramatsu M, Tatematsu M (1997) Reduction of glutathione S-

transferase P-form mRNA expression in remodeling nodules in rat liver revealed by in situ hybridization. Carcinogenesis 18:545–551

Ito N, Tatematsu M, Hasegawa R, Tsuda H (1989) Medium-term bioassay system for detection of carcinogens and modifiers of hepatocarcinogenesis utilizing the GST-P positive liver cell focus as an endpoint marker. Toxicol Pathol 17:630–641

Kato M, Popp JA, Conolly RB, Cattley RC (1993a) Relationship between hepatocyte necrosis, proliferation, and initiation induced by diethylnitrosamine in the male F344 rat. Fundam Appl Toxicol 20:155–162

Kato T, Imaida K, Ogawa K, Hesegawa R, Shirai T, Tatematsu M (1993b) Three-dimensional analysis of glutathione S-transferase placental form-positive lesion development in early stages of rat hepatocarcinogenesis. Jpn J Cancer Res 84:1252–1257

Krutovskikh V (2002) Implication of direct host-tumor intercellular interactions in non-immune host resistance to neoplastic growth. Semin Cancer Biol 12:267–276

Liljegren G, Hardell L, Lindstrom G, Dahl P, Magnuson A (1998) Case-control study on breast cancer and adipose tissue concentrations of congener specific polychlorinated biphenyls, DDE and hexachlorobenzene. Eur J Cancer Prev 7:135–140

Luebeck EG, Buchmann A, Stinchcombe S, Moolgavkar SH, Schwarz M (2000) Effects of 2,3,7,8-tetrachlorodibenzo-p-dioxin on initiation and promotion of GST-P-positive foci in rat liver: a quantitative analysis of experimental data using a stochastic model. Toxicol Appl Pharmacol 167:63–73

Luebeck EG, Grasl-Kraupp B, Timmermann-Trosiener I, Bursch W, Schulte-Hermann R, Moolgavkar SH (1995) Growth kinetics of enzyme-altered liver foci in rats treated with phenobarbital or alpha-hexachlorocyclohexane. Toxicol Appl Pharmacol 130:304–315

Moolgavkar SH, Dewanji A, Venzon DJ (1988) A stochastic two-stage model for cancer risk assessment. I. The hazard function and the probability of tumor. Risk Anal 8:383–392

Moolgavkar SH, Luebeck EG (1992) Interpretation of labeling indices in the presence of cell death. Carcinogenesis 13:1007–1010

Moolgavkar SH, Luebeck EG, Buchmann A, Bock KW (1996) Quantitative analysis of enzyme-altered liver foci in rats initiated with diethylnitrosamine and promoted with 2,3,7,8-tetrachlorodibenzo-p-dioxin or 1,2,3,4,6,7,8-heptachlorodibenzo-p-dioxin. Toxicol Appl Pharmacol 138:31–42

Moolgavkar SH, Luebeck EG, de Gunst M, Port RE, Schwarz M (1990) Quantitative analysis of enzyme-altered foci in rat hepatocarcinogenesis experiments-I. Single agent regimen. Carcinogenesis 11:1271–1278

NTP (2004) Toxicology and carcinogenesis studies of 3,3′,4,4′,5-pentachlorobiphenyl (PCB 126) (CAS No. 57465–28-8) in female Harlan Sprague-Dawley rats (gavage studies). National Toxicology Program, Research Triangle Park, NC

Omori Y, Zaidan Dagli ML, Yamakage K, Yamasaki H (2001) Involvement of gap junctions in tumor suppression: analysis of genetically-manipulated mice. Mutat Res 477:191–196

Ou YC, Conolly RB, Thomas R, Gustafson DL, Long ME, Dovrev ID, Chubb LS, Xu Y, Lapidot S, Andersen ME, Yang RSH (2003) Stochastic simulation of hepatic preneoplasic foci development for four chlorobenzene congeners in a medium-term bioassay. Toxicol Sci 73:301–314

Ou YC, Conolly RB, Thomas RS, Xu Y, Andersen ME, Chubb LS, Pitot HC, Yang RS (2001) A clonal growth model: time-course simulations of liver foci growth following penta- or hexachlorobenzene treatment in a medium-term bioassay. Cancer Res 61:1879–1889

Plante I, Charbonneau M, Cyr DG (2002) Decreased gap junctional intercellular communication in hexachlorobenzene-induced gender-specific hepatic tumor formation in the rat. Carcinogenesis 23:1243–1249

Portier CJ, Sherman CD, Kohn M, Edler L, Kopp-Schneider A, Maronpot RM, Lucier G (1996) Modeling the number and size of hepatic focal lesions following exposure to 2,3,7,8-TCDD. Toxicol Appl Pharmacol 138:20–30

Saltykov SA (1967) The determination of the size distribution of particles in an opaque material from a measurement of the size distribution of their sections. In: Elias H (ed) Proceedings of the second international congress for stereology, Chicago, April 8–13. Springer, Berlin, pp 163–173

Satoh K, Hatayama I, Tateoka N, Tamai K, Shimizu T, Tatematsu M, Ito N, Sato K (1989) Transient induction of single GST-P positive hepatocytes by DEN. Carcinogenesis 10:2107–2111

Smith AG, Francis JE, Dinsdale D, Manson MM, Cabral JR (1985) Hepatocarcinogenicity of hexachlorobenzene in rats and the sex difference in hepatic iron status and development of porphyria. Carcinogenesis 6:631–636

Thomas RS (1998) The use of biologically-based models for integrating short-term cancer bioassays, mechanisms of action, and target tissue dosimetry: application to pentachlorobenzene. Ph.D. Dissertation, Department of Environmental Health, Colorado State University, Ft. Collins

Thomas RS, Conolly RB, Gustafson DL, Long ME, Benjamin SA, Yang RS (2000) A physiologically based pharmacodynamic analysis of hepatic foci within a medium-term liver bioassay using pentachlorobenzene as a promoter and diethylnitrosamine as an initiator. Toxicol Appl Pharmacol 166:128–137

Weibel ER, Staubli W, Gnagi HR, Hess FA (1969) Correlated morphometric and biochemical studies on the liver cell. I. Morphometric model, stereologic methods, and normal morphometric data for rat liver. J Cell Biol 42:68–91

Xu YH, Pitot HC (2003) An improved stereologic method for three-dimensional estimation of particle size distribution from observations in two dimensions and its application. Comput Methods Programs Biomed 72:1–20

Yang RSH (1994) Introduction to the toxicology of chemical mixtures. In: Yang RSH (ed) Toxicology of chemical mixtures: case studies, mechanisms, and novel approaches. Academic, San Diego, pp 1–10

Yang RSH (1997) Toxicologic interactions of chemical mixtures. In: Bond J (ed) Comprehensive toxicology, Vol. 1, General principles, toxicokinetics, and mechanisms of toxicity. Elsevier, Oxford, pp 189–203

Yusuf A, Rao PM, Rajalakshmi S, Sarma DS (1999) Development of resistance during the early stages of experimental liver carcinogenesis. Carcinogenesis 20:1641–1644